ARTICLE

Study on Factors Affecting Properties of Foam Glass Made from Waste Glass

Yang Liu[1], Jianjun Xie[1,*], Peng Hao[1], Ying Shi[1], Yonggen Xu[2,3] and Xiaoqing Ding[2,3]

[1]School of Material Science and Engineering, Shanghai University, Shanghai, China

[2]Huichang New Material Co., Ltd., Xuancheng, China

[3]Changda Thermal Insulation Technology Co., Ltd., Xuancheng, China

[*]Corresponding Author: Jianjun Xie. Email: xiejianjun@shu.edu.cn

ABSTRACT

Foam glass is a new green material to make use of waste glass and is popular for its energy-saving and light weight features. The problems in the current study of foam glass is that its properties require improvement to match the growing demands of application specific standards. Properties of foam glass is related to its porous structure, which is affected by various factors. The influence of raw material component, foaming agents and sintering system on the porous structure and properties of foamed glass is studied. Density decreases with the decrease of quartz and barite content. Thermal conductivity is more affected by barite content, and the lowest thermal conductivity is obtained when 10% quartz and 6% borax are added. Compressive strength is more affected by borax content, and the highest compressive strength is obtained when 5% quartz, 10% barite and 6% borax are added. Foam glass samples with different porous structures and improved properties are obtained using graphite and $CaCO_3$ as foaming agents. Compared with the soldcommercial foam glass for thermal insulation materials, the compressive strength of samples prepared by using compound foaming agents is increased by a factor of 2–3 times higher. With porous structure and properties adjusted by the optimization of raw materials and foaming agent, there exists the potential for factories to produce foam glass with expanded application scope.

KEYWORDS

Foam glass; waste glass; orthogonal test; properties

1 Introduction

With the continuous promotion of environmental protection policies, green and environmentally friendly materials are more attractive to users in various fields [1–3]. Foam glass, a new green material made from waste, has a highly porous structure (total porosity > 80%). Properties and application of foam glass depend on its pore type. Closed-porous foam glass (open porosity < 10%) applies to building material and has superior performance over traditional thermal insulation materials, including low thermal conductivity ($\lambda < 0.1$ W·m^{-1}·k^{-1}), high compressive strength ($\sigma > 0.5$ MPa), water resistance and long life-span. Open-porous foam glass (open porosity > 50%) shows good sound insulation and water absorption capability, applying in metro station and gardens.

The main raw materials for foam glass are waste including types of waste glass, fly ash and slag [4–8]. New raw materials for foam glass producing appear in recent years [9,10]. As reported, according to chemical composition of the raw materials [11], the foaming agent, which releases gas bubbles in the softened glass or a slag powder to form a porous structure, is selected to match the thermal properties of the raw materials. Of all the published decomposition and redox reaction type foaming agents, black carbon is the most commonly used and the gas released (CO_2) by it has a lower thermal conductivity than N_2 and O_2 [12,13]. Different raw material components, foaming agents, auxiliary agent types, and sintering or annealing process all lead to a different porous structure and foam glass performance. Apart from low apparent density, foam glass with predominantly closed pores exhibits low thermal conductivity and high water resistance, while that with predominantly open pores exhibits excellent acoustic insulation.

Despite the fact that foam glass appeared in the 1940s, companies and literature reports only began to grow substantially in the past 10 years. With the rapid development of foam glass industry, the problems of overcapacity and backward performance have emerged. Recently, foam glass is mainly used as a thermal or acoustic insulation material because of its highly porous structure [14]. Compared with traditional thermal insulation materials, foam glass has a much longer lifespan resulting from its chemical and thermal stability. However, compressive strength should also be considered in all application fields [15]. The compressive strength of foam glass is related to its porous structure, which is affected by a large number of factors [16,17]. Firstly, due to the difference between foaming temperatures of various foaming agents [18,19], the viscosity of the melt during the foaming stage differs [20], thus, the resulting resistance to pore growth differsAdditionally, particle size affects the uniformity of the foaming agents in the mixture and the severity of the foaming reaction [12]. Inhomogeneous dispersion of the foaming agent and an incomplete foaming reaction lead to a non-uniform porous structure foam glass with reduced compressive strength [21]. Further, during the foam glass sintering process, pore coalescence is enhanced by prolonging the holding time or increasing the cooling rate [4], forming a predominantly open-porous distribution, which leads compressive strength to decrease.

Since the formation of foam glass is complex, the understanding of factors affecting structure and properties of foam glass makes it possible that porous structure and properties of foam glass are adjusted to meet different application standards. The present work is twofold: (i) To study the influence of raw material content on structure and properties of foam glass by the orthogonal test. Considering quartz sand, barite and borax content as the main factors, an orthogonal experiment having three factors divided into three levels is designed. (ii) To study the influence of different types of foaming agentson structure and properties of foam glass. Graphite is a redox foaming agent, which can produce gas continuously during the heating process, and is likely to form a closed-porous structure [18]. $CaCO_3$ is a decomposition foaming agent, which decomposes at high temperature, producing large volumes of gas, and is thus likely to form an open-porous structure [22]. $CaCO_3$ is added to couple with graphite to form compound foaming agents. By altering the raw material content, proportion of compound agents, and the foaming temperature, the pore structure of foam glass can be adjusted and its properties optimized. Thus, the performance requirements of foam glass in different service fields can be met, expanding the application scope of foam glass.

2 Experiment

Waste glass was crushed into pieces by a hammer and subsequently ball milled with ethanol in a planetary ball for 3 hours at 200 rpm. The obtained powders were then dried for 2 hours. Graphite (CP, Sinopharm) and calcium carbonate (CP, Sinopharm) were added to the fine glass powder and were ball milled at 150 rpm for 45 min. Graphite and $CaCO_3$ powders were ball milled first to form big aggregate before added to the whole mixture,their main reactions during foaming process are listed below. The powder mixtures were placed in a stainless steel mold coated with a release agent and heated at 10°C/min

to different foaming temperature. Subsequently, the sample was cooled at 5°C/min to the glass transition temperature and then naturally cooled to room temperature. Obtained sample was processed to square shape and kept in oven.

$$C + O_2 \rightarrow CO_2 \tag{1-1}$$

$$C + H_2O \rightarrow H_2 + CO \tag{1-2}$$

$$C + CO_2 \rightarrow 2CO \tag{1-3}$$

$$CaCO_3 \rightarrow CaO + CO_2 \uparrow \tag{1-4}$$

$$CaCO_3 + SiO_2 \rightarrow CaSiO_3 + CO_2 \uparrow \tag{1-5}$$

Waste glass powder was heated to 300°C to eliminate polymer impurities and then the chemical composition of the float glass powder was obtained by chemical analysis with an X-ray fluorescence spectrometer (XRF-1800, SHIMADZU LIMITED, Japan).

The morphology of foam glass was examined using a scanning electron microscope (SEM) operating at 15 kV (Nova NanoSEM 450, FEI, CZ). SEM measurements were performed on powder mixtures coated with Au.

X-ray diffraction analysis (XRD) was performed with an X-ray diffractometer 3KW D/MAX2200V PC (Riken Electric Co., Ltd., Japan).

To investigate the thermal activities of foaming agents during the heating process, differential scanning calorimetry (DSC) and thermogravimetry (TG) measurements were performed using a synchronous thermal analyser 404C instrument (NETZSCH-Gerätebau GmbH, Germany).

Shown in Fig. 1, the thermal conductivity of the prepared samples ($12 \times 12 \times 1.5$ mm^3) at room temperature was investigated using the transient hot line method (TC3000E, XIATECH, China). For this purpose, the sensor is sandwiched between two flat test specimens and pressed with a 500 g weight to reduce the thermal contact resistance generated by air. The sensor was electrically heated by applying a specific constant heating power at 0.5–4.5 V over a defined measuring time of 1–30 s [9]. By measuring the increase in the electrical resistance, the temperature increase of the wire was determined, which is directly related to the thermal conductivity of the sample [18]. Theoretical calculation formula of thermal conductivity model for foamed glass is [23]:

$$\lambda = \frac{2}{3}\lambda_s P_s + \lambda_p P_p \tag{2-1}$$

λ_s—thermal conductivity of basic glass

P_s—volume of glass phase

λ_p—thermal conductivity of gas

P_p—volume of gas phase

The compressive strength of the prepared samples ($12 \times 12 \times 1.5$ mm^3) was investigated with a universal material testing machine (JWE-50, China). The true density (ρ_t) was determined by Archimedes' principle using a complete float glass block. The apparent densities (ρ_{app}) of the small samples were determined by Archimedes' principle using a density weighing balance. The apparent density (ρ_{app}) of the large samples was calculated from the mass and dimensions of the sample [24]. Additionally, the percentages of total porosity (TP), open porosity (OP) and closed porosity (CP) were calculated from m_1 (dry weight), m_2 (wet weight), m_3 (absorbed water weight).

Figure 1: Picture of sensor for transient hot line method

$$\rho_{app} = \frac{m_1}{m_3 - m_2}; \quad OP = \frac{m_3 - m_1}{m_3 - m_2}; \quad TP = 1 - \frac{\rho_{app}}{\rho_t}; \quad CP = 1 - \frac{OP}{TP} \tag{3-1}$$

Theoretical calculation formula of strength model for porous materials is [25]:

$$\frac{R}{R_0} = 1 - 1.209 Z_h V_p^{\frac{2}{3}} \tag{4-1}$$

$$Z_h = \sum_{i=0}^{n} m_i k_{i+1} P_{n-i}^2 \left(\sum_{i=0}^{n} m_i k_{i+1} P_{n-i}^3 \right)^{-\frac{2}{3}} \tag{4-2}$$

R—strength of porous materials

R_o—strength of solid materials

Z_h—constant determined by pore size

m—number of pores

k—ratio of major axis to minor axis of ellipsoidal hole

p—pore size

V_p—volume of gap

The mean pore size and pore size dispersion were calculated from the macrostructure of the prepared samples using analysis software (Nanomeasure). The calculation process is shown in Fig. 2.

3 Results and Discussion

3.1 material Characterization

As shown in Tab. 1, waste glass has a large amount of CaO and Na_2O content, which reduces the melting point. When quartz and barite are added, increase of high melting point component enhance the lattice strength of glass, making bubbles more stable during sintering process.
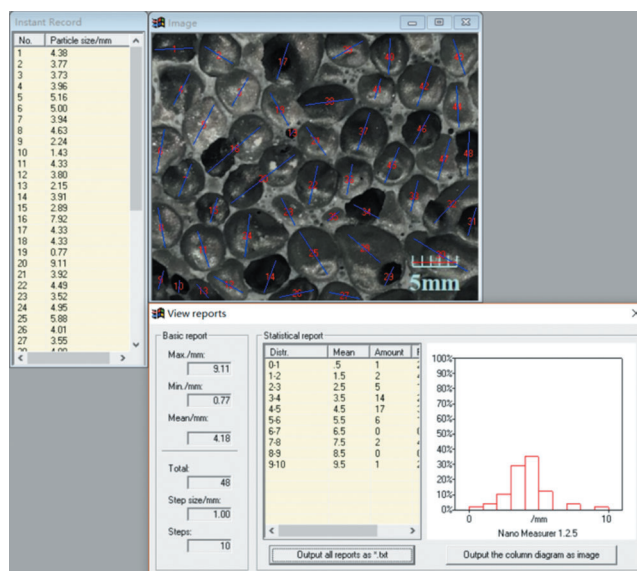
Figure 2: Nanomeasure software calculation process

Table 1: Raw material chemical composition determined by X-ray fluorescence

Waste glass	SiO_2	CaO	Na_2O	MgO	Al_2O_3	K_2O	other
	67.87%	14.38%	11.59%	4.19%	0.83%	0.40%	0.74%
Quartz	SiO_2	Al_2O_3	CaO	Fe_2O_3	K_2O		
	83.85%	14.95%	0.69%	0.37%	0.13%		
Barite	SiO_2	BaO	SO_3	Fe_2O_3	Al_2O_3	K_2O	other
	59.06%	24.02%	7.11%	3.17%	2.24%	0.69%	3.70%

TG-DSC result of waste glass is shown in Fig. 3. Since Tg of waste glass is around 700°C, $CaCO_3$ (start to generate CO_2 at around 800°C) and graphite (start to generate CO_2 at around 600°C) is used in the present work, which better fits the muffle furnace's intermittent heating program features and avoid the leak of CO_2 during the pre-sintering stage (400°C–550°C).
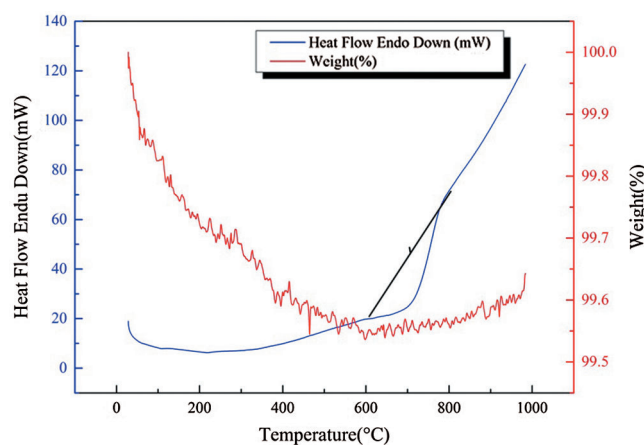
Figure 3: Thermogravimetry-differential scanning calorimetry (TG-DSC) curves of waste glass

3.2 Orthogonal Test Results

Apart from difference of raw material and borax content, Sample (a)-(i) are all made by $CaCO_3$ foaming agents sintered at 850°C. Density, thermal conductivity and compressive strength values are listed in Tab. 2.

The range analysis result is listed in Tab. 3.

Table 2: Orthogonal test results of combined raw materials[a]

Sample	Waste glass/(%)	A Quartz /(%)	B Barite /(%)	C Borax /(%)	Density /(g/cm³)	Open porosity/(%)	λ/ (Wm^{-1}K^{-1})	σ/ (MPa)
(a)	100	1(0)	1(0)	1(2)	0.283	6.78	0.053	0.541
(b)	90	2(5)	2(5)	1(2)	0.485	38.9	0.068	0.692
(c)	80	3(10)	3(10)	1(2)	0.527	15.1	0.060	1.101
(d)	85	3(10)	2(5)	2(4)	0.541	9.46	0.070	0.806
(e)	95	2(5)	1(0)	2(4)	0.271	10.8	0.044	2.130
(f)	90	1(0)	3(10)	2(4)	0.439	22.2	0.091	0.812
(g)	95	1(0)	2(5)	3(6)	0.348	10.7	0.099	3.701
(h)	85	2(5)	3(10)	3(6)	0.469	10.1	0.126	5.160
(i)	90	3(10)	1(0)	3(6)	0.305	5.79	0.052	0.901

[a]Total mass of waste glass, quartz and barite is 5 g (100%). λ is thermal conductivity. σ is compressive strength.
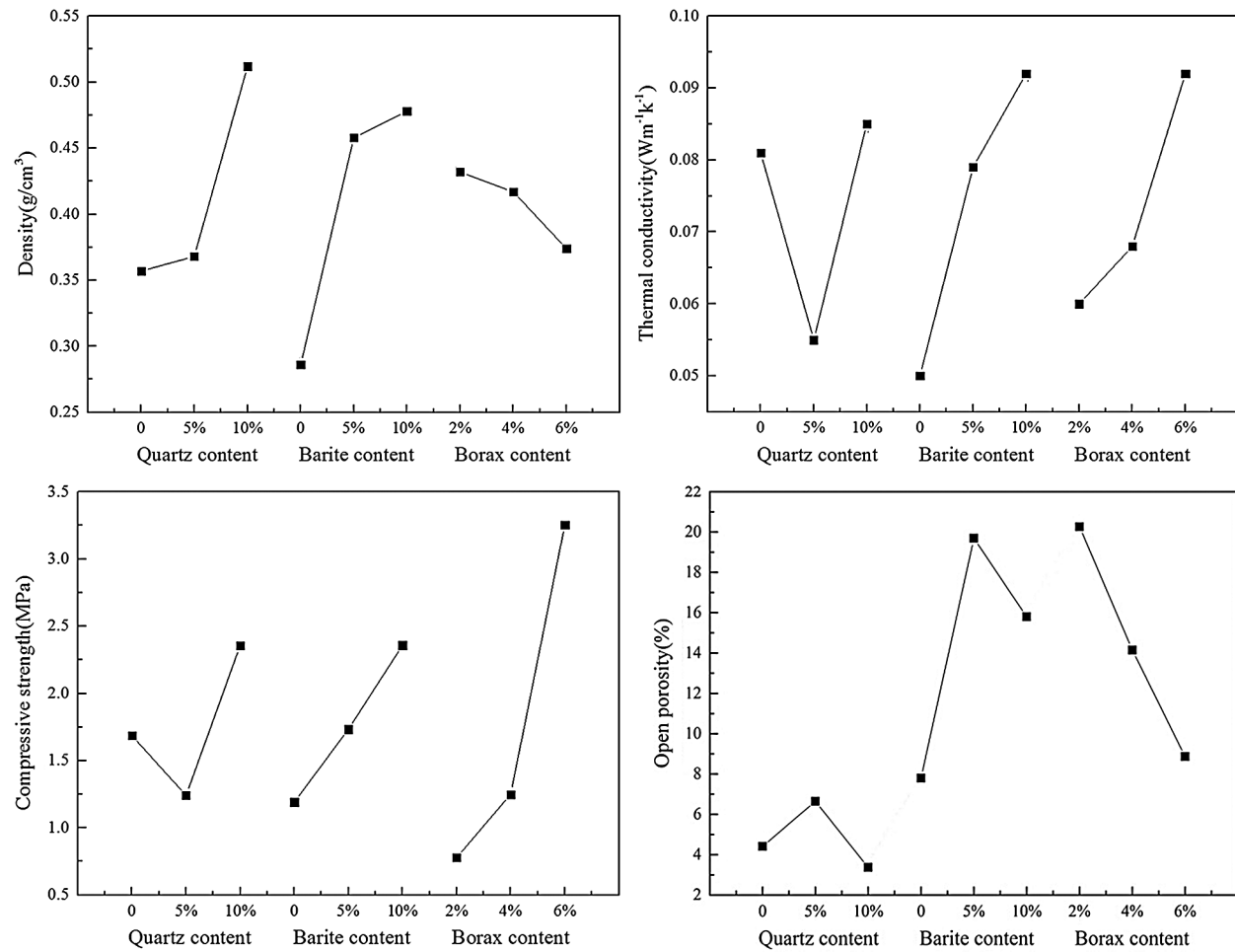
Table 3: Range analysis of orthogonal test results

Index	Density			λ			σ			Open porosity		
	A	B	C	A	B	C	A	B	C	A	B	C
$K1_j$	1.070	0.859	1.295	0.243	0.149	0.181	5.054	3.572	2.334	13.23	23.37	60.78
$K2_j$	1.104	1.374	1.251	0.164	0.237	0.205	3.723	5.199	3.748	19.93	59.06	42.46
$K3_j$	1.537	1.435	1.122	0.256	0.277	0.277	7.067	7.073	9.762	10.12	47.40	26.59
$k1_j$	0.357	0.286	0.432	0.081	0.050	0.060	1.685	1.191	0.778	4.410	7.790	20.26
$k2_j$	0.368	0.458	0.417	0.055	0.079	0.068	1.241	1.733	1.249	6.643	19.69	14.15
$k3_j$	0.512	0.478	0.374	0.085	0.092	0.092	2.356	2.358	3.254	3.373	15.80	8.863
R_j	0.155	0.192	0.058	0.030	0.042	0.032	1.115	1.167	2.476	3.270	11.90	11.40

Fig. 4 is based on k_j value in Tab. 3. As Fig. 4 shows, According to the thermal conductivity and strength model of porous materials, thermal conductivity increases with glass phase volume, while compressive strength increases with uniform porous structure and decrease of gap volume when total porosity remains unchanged. With the increase of quartz content (0–5%), density and open porosity increases slowly, while thermal conductivity and compressive strength decrease, indicating that uniformity decreases and gap volume increases with increase of open porosity. With more quartz added (5%–10%), increase of glass phase and growth resistance lead to the increase of thermal conductivity and compressive strength and decrease of open porosity. Density, thermal conductivity and compressive strength increase with barite content, but open porosity decreases when barite increases from 5% to 10%, indicating the collapse of big pores. With the increase of borax content (decompose to Na_2O and B_2O_3 at high temperature),

fluxing effect of Na_2O and enhancement of glass lattice strength by B_2O_3 lead to the decrease of density and open porosity.

It can be seen from Tab. 4 that the F of the three factors is below the critical value of density, thermal conductivity and compressive strength. Comparing F values, quartz has the greatest influence on density and borax has the greatest influence on thermal conductivity and compressive strength.

Figure 4: Curve of range analysis of orthogonal test results

Table 4: Variance analysis of orthogonal test results

Performance index	Variance source	Sum of squares	Df	Mean value	F	Critical value	Significance
Density	A	0.014	2	0.007	2.999	$F_{0.01}(2,2) = 99.0$	**
	B	0.032	2	0.016	6.660	$F_{0.05}(2,2) = 19.0$	***
	C	0.005	2	0.003	1.139	$F_{0.10}(2,2) = 9.0$	*
	Residual	0.005	2	0.002			
	Σ	0.056	8				

(Continued)

Table 4 (continued).

Performance index	Variance source	Sum of squares	Df	Mean value	F	Critical value	Significance
Thermal conductivity	A	0.000	2	0.000	0.288	$F_{0.01}(2,2) = 99.0$	*
	B	0.001	2	0.001	1.641	$F_{0.05}(2,2) = 19.0$	**
	C	0.002	2	0.001	1.871	$F_{0.10}(2,2) = 9.0$	***
	Residual	0.001	2	0.000			
	Σ	0.004	8				
Compressive strength	A	0.330	2	0.165	0.040	$F_{0.01}(2,2) = 99.0$	*
	B	0.490	2	0.245	0.059	$F_{0.05}(2,2) = 19.0$	**
	C	10.381	2	5.191	1.245	$F_{0.10}(2,2) = 9.0$	***
	Residual	8.336	2	4.168			
	Σ	19.537	8				

Therefore, when preparing foam glass for use of thermal insulation material, barox content is considered first to get a uniform porous structure and fine thermal and mechanical properties. Quartz and barite content are considered second to get a lower density and higher compressive strength.

3.3 Micromorphology of Foam Glass Samples Made by Combined Raw Materials

It can be seen from Fig. 5 sample (a) and (b) that a few large pores are surrounded by a number of small pores. These small pores are referred to as a bubble band because of their bubble like features and continuous distribution [16]. In the process of bubble growth, the existence of bubble bands reduces the gap volume, thus, enhances the strength of large pores Sample (a) has an inhomogeneous porous structure and the bubble band is cut off by large pores. An indentation within a large pore is seen in samples (b) and (i), but no coalescence of pores has occurred. Sample (c) and (h) show a homogeneous porous structure with thick pore walls, while pore walls are thin and sharp in samples (d) and (e). Coalescence and collapse of pores are evident in samples (e) and (f). Sample (h) has the highest compressive strength of 5.16 MPa. The SEM micrograph shows a homogeneous porous structure with thin pore walls.

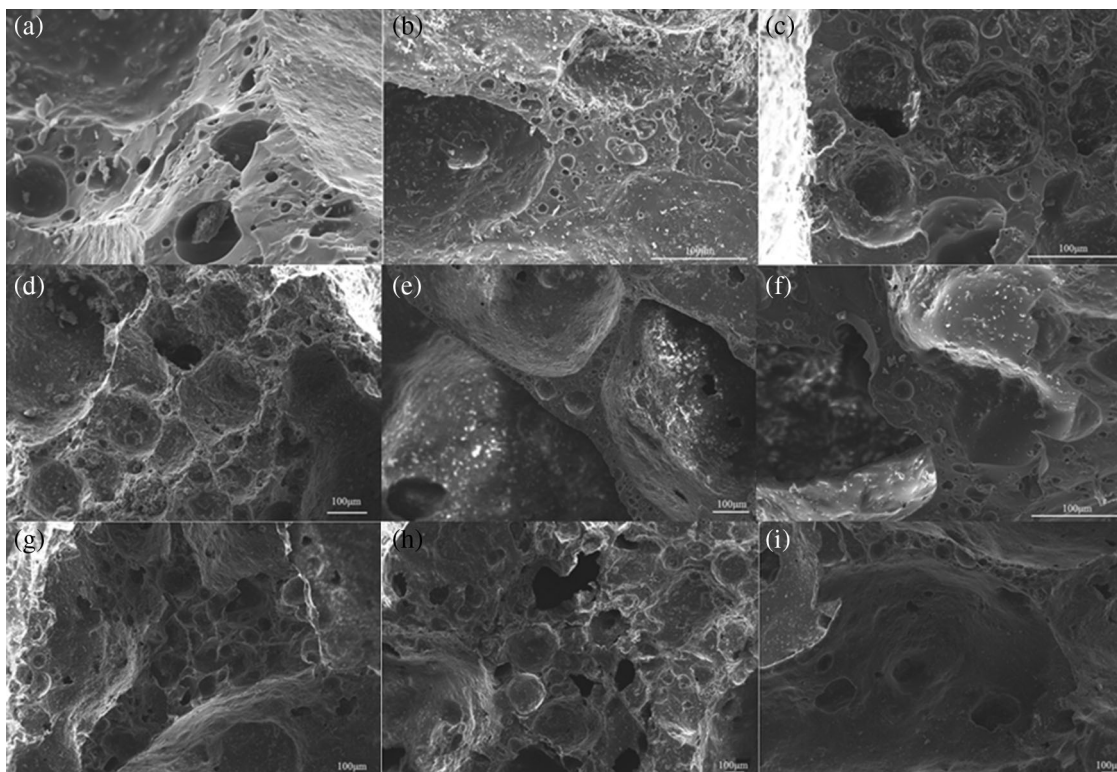### 3.4 XRD Analysis of Foam Glass Samples Made by Combined Raw Materials

The results (Fig. 6) show that the diffraction peak of quartz is very weak in sample (a), in which only waste glass is used. When the ratio of quartz sand and barite added to the raw materials is 1:1, a high intensity quartz peak is seen in samples (b) and (c). The raw materials of sample (g) and sample (f) are waste glass and barite. A high intensity $BaSO_4$ peak is seen in sample (g), indicating that increase of borax from 4% to 6% lead to the crystallization of $BaSO_4$.

Based on the above results, the optimal raw material proportions for subsequent experiments are 95% waste glass, 5% quartz and 2% borax.

3.5 Micromorphology of Foam Glass Samples Made by Compound Foaming Agents

Figs. 7a and 7b are micrographs of foam glass samples prepared with graphite foaming agents. Fig. 7b shows that there are some tiny pores inside larger pores, indicating that growth resistance differs in different directions. Fig. 7d shows that when $CaCO_3$ is added, most pores grow bigger and large pores surrounded by bubble band are mostly closed. Fig. 7c shows that when more $CaCO_3$ is added, the wall between pores becomes too thin for bubble bands to exist, and most pores are connected which leads to a decrease in compressive strength.

Figure 5: SEM micrographs of foam glass samples made using combined raw materials. All scale bars 100 µm
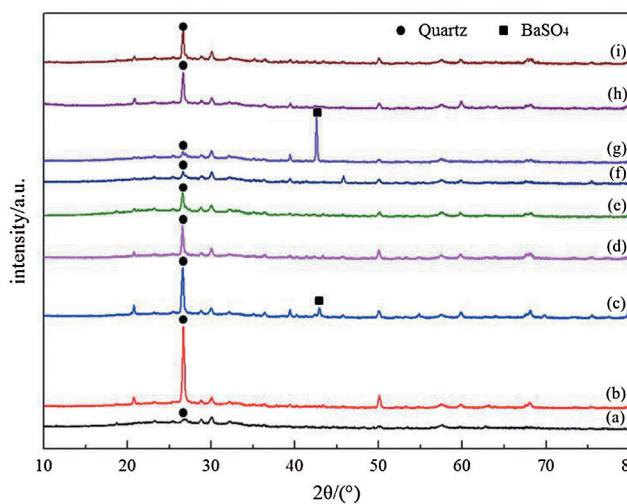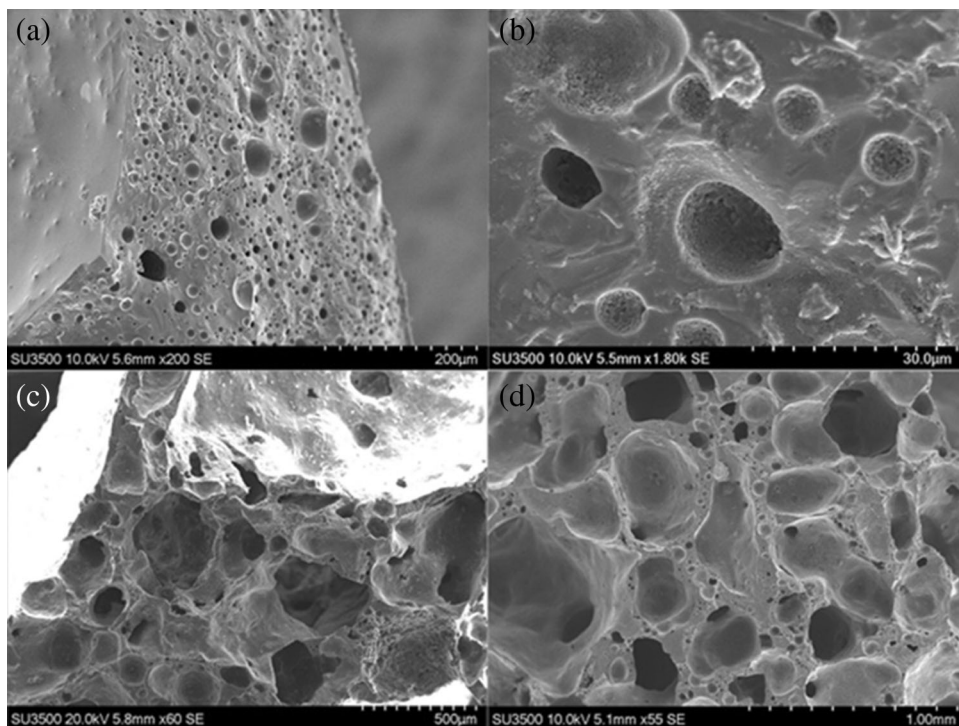

Figure 6: X-ray diffraction patterns of foam glass prepared from combined raw materials

3.6 XRD Analysis of Foam Glass Samples Made by Compound Foaming Agents

As the XRD analysis results of Fig. 8 show, a sharp graphite diffraction peak ($2\theta = 26.546°$) is detected when the foaming agent is 1% graphite. This is because when the mixture is heated above the glass transition temperature, the graphite particles are gradually surrounded by the liquid phase, and the oxygen between the particles is not sufficient to allow the graphite to react completely. With the addition of $CaCO_3$, which decomposes at high temperature and releases a large amount of CO_2, residual graphite is consumed

through reaction (1–3), resulting in a weak graphite diffraction peak. As the content of $CaCO_3$ is increased from 1% to 3%, the graphite diffraction peak is unchanged, but an enhancement of the silicon oxide diffraction peak ($2\theta = 30.104°$) was observed. This may be the superposition of the $CaSiO_3$ diffraction peak ($2\theta = 29.975°$) and the silicon oxide diffraction peak, caused by some of the aggregate $CaCO_3$ following reaction (1–5), and crystallization of $CaSiO_3$ occurring.


Figure 7: SEM micrograph of foam glass sample section for (a), (b) 1% graphite, (c) 1% graphite and 2% $CaCO_3$ and (d) 1% graphite and 1% $CaCO_3$. Micrographs not to the same scale
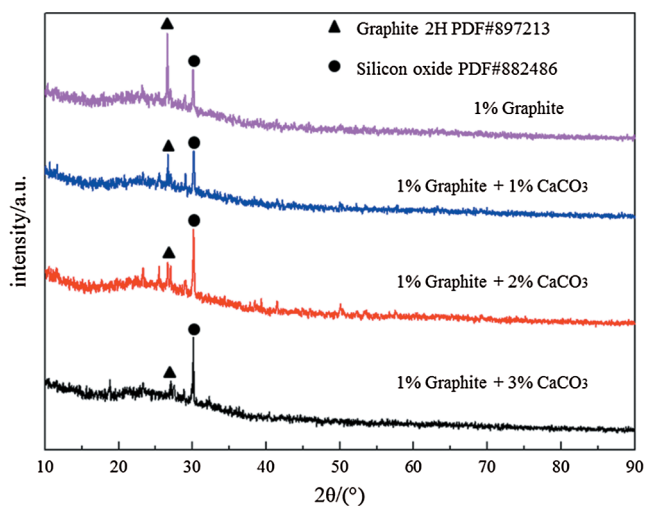
Figure 8: X-ray diffraction patterns of foam glass prepared with compound foaming agents
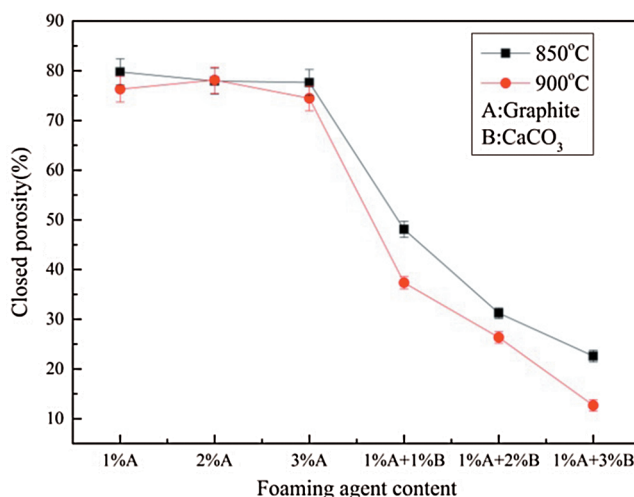
3.7 Effect of Foaming Agent Content and Foaming Temperature on Pore Structure of Foam Glass Samples

Fig. 9 shows that the total porocity of foam glass samples increases slowly as the amount of graphite is increased and as the foaming temperature is increased. The TG-DSC curve (Fig. 3) shows that Tg of waste glass is 737.66°C. Graphite starts to react at about 600°C when the glass matrix is not completely melted and CO_2 can easily escape. Additionally, the oxygen content in the pores of the glass matrix is low at high temperature, and graphite is relatively stable and difficult to oxidize. Thus, the low expansion of foam glass leads to a low total porocity. For compound foaming agents, the total porosity of the foam glass samples increased rapidly. With the increase of $CaCO_3$ content and foaming temperature, the sample total porocity further increased to 90.13%. This is because the decomposition of $CaCO_3$ at high temperature produces large amounts of CO_2, and CaO breaks the tetrahedral structure of SiO_2 to reduce the resistance of pore growth [24].
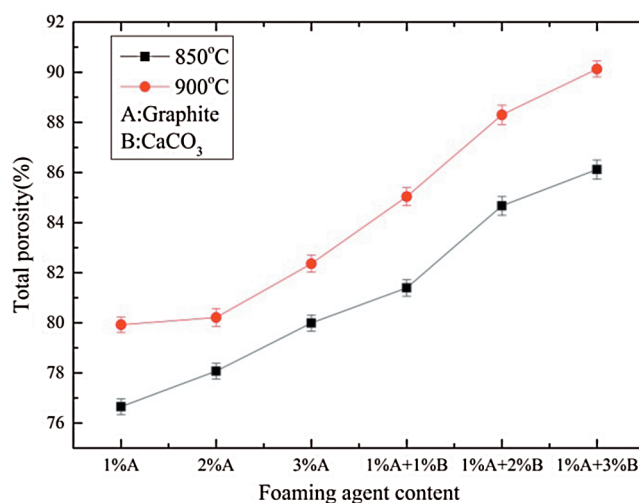

Figure 9: Total porosity as a function of foaming agent content and foaming temperature

As shown in Fig. 10, even for increased foaming temperature and foaming agent content, the porosity of foam glass prepared by a single foaming agent remains at 70%–80%. When graphite and $CaCO_3$ are used in combination, closed pores decrease from 80% to 10% porosity. This is a practical means to adjust the closed porosity of foam glass, meeting the requirement of different application fields [14,26].

Figure 10: Closed porosity of foam glass samples as a function of foaming agent content and foaming temperature
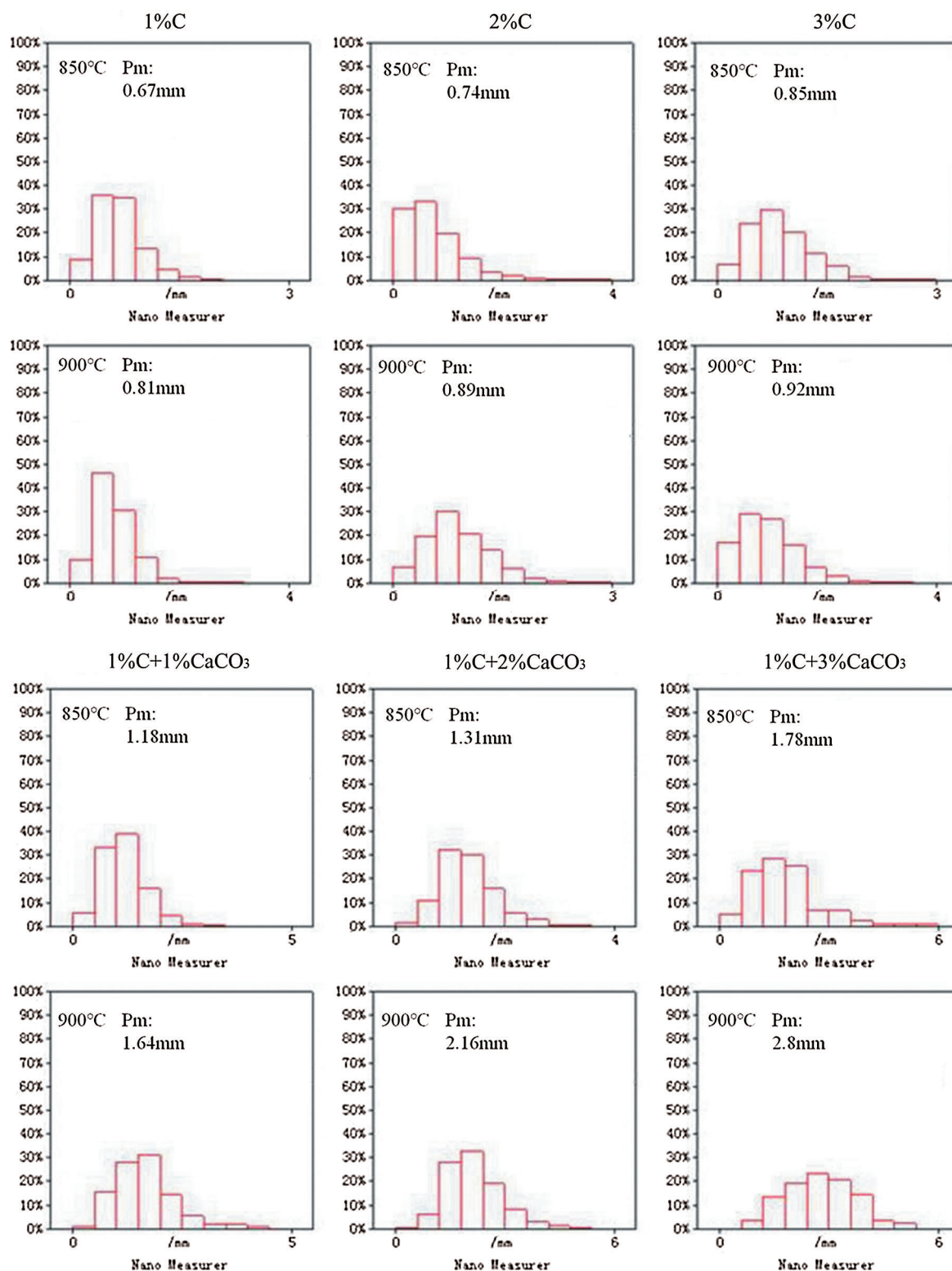
Figure 11: Pm (mean pore size) of foam glass made using different foaming agents

It can be seen from the foam glass pore distribution map (Fig. 11) that the mean pore size of foam glass prepared using a single foaming agent is small, and the pore growth is not related to the increase of graphite content and foaming temperature. The proportion of pores below 1 mm decreased, and the mean pore size of foam glass increased with the increase of $CaCO_3$ content.
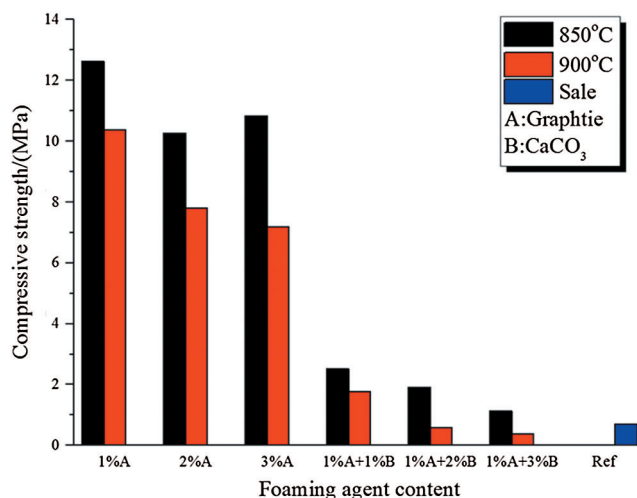
3.8 Effect of Foaming Agent Content and Foaming Temperature on Thermal Conductivity and Compressive Strength of Foam Glass Samples

It can be seen from Fig. 12 that increasing the foaming agent content and foaming temperature reduces the thermal conductivity of foam glass, and that the thermal conductivity is more sensitive to the change of foaming temperature than foaming agent content. The thermal conductivity of foam glass prepared using a compound foaming agent meets the thermal performance requirements of insulation material. The obtained lowest thermal conductivity is 0.0516 ($W \cdot m^{-1} K^{-1}$), which is lower than that of commercial foam glass. With increasing of $CaCO_3$ content, the rate of change of thermal conductivity decreases. This is because increasing the number of open pores leads to an increase of gas flow heat transfer and gas-solid convection heat transfer [4]. Thus, in order to obtain further decrease of thermal conductivity, a larger closed porosity must be achieved without decreasing the total porosity.
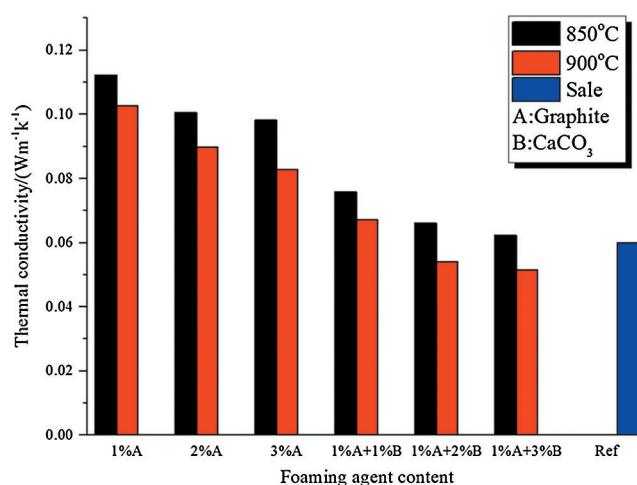
Figure 12: Histogram showing effect of foaming agent content and temperature on thermal conductivity of foam glass samples

It can be seen from Fig. 13 that graphite plays an important role in increasing the compressive strength of foam glass when using compound foaming agents. Samples made using 1% graphite coupled with 2% or 3% $CaCO_3$ at 850°C, have a thermal conductivity close to that of commercial foam glass but with a 59%–169% increase in compressive strength.

Figure 13: Histogram showing effect of foaming agent content and temperature on compressive strength of foam glass samples

4 Conclusion

In summary based on the above experiments we conclude:

i)   According to the results of the orthogonal test, porous structure and properties are adjusted by change of raw materials. It is practical to improve foam glass quality used as thermal insulation materials. barox content is considered first to get a uniform porous structure and fine thermal and mechanical properties. Quartz and barite content are considered second to get a lower density and higher compressive strength.

ii) CO_2 produced by decomposition of $CaCO_3$ at high temperature reacts with graphite, making the oxidation of graphite more complete to increase growth motivate power of pores. The residual graphite is distributed on the phase interface of gas and liquid phase, which reduces the interface energy and stabilize the pores, thus, foaming a highly porous structure with good compressive strength. Foam glass with optimized performance is obtained by 1% graphite and 2% $CaCO_3$ at 850°C, which exhibits insulation performance ($\lambda = 0.0661 W \cdot m^{-1} \cdot k^{-1}$) as good as commercial foam glass with much better mechanical performance (218% improvement).

iii) With the increase of $CaCO_3$ content, porous structure changes from closed-porosity to open-porosity. It is practical for foam glass to meet application specific porous structure requirements, such as those of sound insulation materials and water storaging materials.

Conflicts of Interest: The authors declare that they have no conflicts of interest to report regarding the present study.

References

1. Lebullenger, R., Chenu, S., Rocherullé, J., Merdrignac-Conanec, O., Cheviré, F. et al. (2010). Glass foams for environmental applications. *Journal of Non-Crystalline Solids, 356(2),* 2562–2568. DOI 10.1016/j.jnoncrysol.2010.04.050.

2. König, J., Lopez, G. A., Cimavilla, R. P., Rodriguez-Perez, M. A., Petersen, R. R. et al. (2020). Synthesis and properties of open- and closed-porous foamed glass with a low density. *Construction and Building Materials, 247(3),* 121–124.

3. Caniato, M., D'Amore, G. K. O., Kaspar, J., Gasparella, A. (2019). Application of analytical and numerical tools for the optimization of forecasting models. *Applied Acoustics, 161.* DOI 10.1016/j.apacoust.2019.107166.

4. König, J., Petersen, R., Yue, Y. (2015). Fabrication of highly insulating foam glass made from CRT panel glass. *Ceramics International, 41(8),* 9793–9800. DOI 10.1016/j.ceramint.2015.04.051.

5. Fernandes, H. R., Andreola, F., Barbieri, L., Lancellotti, I., Pascual, M. J. et al. (2013). The use of egg shells to produce Cathode Ray Tube (CRT) glass foams. *Ceramics International, 39(8),* 9071–9078. DOI 10.1016/j.ceramint.2013.05.002.

6. Chen, B., Luo, Z., Lu, A. (2011). Preparation of sintered foam glass with high fly ash content. *Materials Letters, 65 (23–24),* 3555–3558. DOI 10.1016/j.matlet.2011.07.042.

7. Ewais, E. M. M., Attia, M. A. A. , El-Amir, A. A. M., Elshenway, A. M. H., Fend, T. et al. (2018). Optimal conditions and significant factors for fabrication of soda lime glass foam from industrial waste using nano AlN. *Journal of Alloys and Compounds, 747(2),* 408–415. DOI 10.1016/j.jallcom.2018.03.039.

8. Guo, H. W., Gong, Y. X., Gao, S. Y. (2010). Preparation of high strength foam glass–ceramics from waste cathode ray tube. *Materials Letters, 64(8),* 997–999. DOI 10.1016/j.matlet.2010.02.006.

9. Hesky, D., Aneziris, C. G., Groß, U., Horn, A. (2015). Water and waterglass mixtures for foam glass production. *Ceramics International, 41(10),* 12604–12613. DOI 10.1016/j.ceramint.2015.06.088.

10. Ji, R., Zheng, Y., Zou, Z., Chen, Z. W., Wei, S. et al. (2019). Utilization of mineral wool waste and waste glass for synthesis of foam glass at low temperature. *Construction and Building Materials, 215(3),* 623–632. DOI 10.1016/j.conbuildmat.2019.04.226.

11. König, J., Petersen, R. R., Iversen, N., Yue, Y. Z. (2018). Suppressing the effect of cullet composition on the formation and properties of foamed glass. *Ceramics International, 44(10),* 11143–11150. DOI 10.1016/j.ceramint.2018.03.130.

12. König, J., Petersen, R. R., Yue, Y. Z. (2016). Influence of the glass particle size on the foaming process and physical characteristics of foam glasses. *Journal of Non-Crystalline Solids, 447(2),* 190–197. DOI 10.1016/j.jnoncrysol.2016.05.021.

13. Petersen, R. R., König, J., Smedskjaer, M. M. (2014). Foaming of CRT panel glass powder using Na_2CO_3. *Glass Technology-European Journal of Glass Science and Technology Part A, 55(1),* 1–6.

14. Kyaw, O., Caniato, G., Travan, M., Turco, A., Marsich, G. et al. (2017). Innovative thermal and acoustic insulation foam from recycled waste glass powder. *Journal of Cleaner Production, 165(3),* 1306–1315. DOI 10.1016/j.jclepro.2017.07.214.

15. Qu, Y., Xu, J., Su, Z., Ma, N., Zhang, X. Y. et al. (2016). Lightweight and high-strength glass foams prepared by a novel green spheres hollowing technique. *Ceramics International, 42(2),* 2370–2377. DOI 10.1016/j.ceramint.2015.10.034.

16. Korat, L., Ducman, V., Legat, A., Mirtič, B. (2013). Characterisation of the pore-forming process in lightweight aggregate based on silica sludge by means of X-ray micro-tomography (micro-CT) and mercury intrusion porosimetry (MIP). *Ceramics International, 39(6),* 6997–7005. DOI 10.1016/j.ceramint.2013.02.037.

17. Ducman, V., Korat, L., Legat, A., Mirtič, B. (2013). X-ray micro-tomography investigation of the foaming process in the system of waste glass–silica mud–MnO_2. *Materials Characterization, 86(2),* 316–321. DOI 10.1016/j.matchar.2013.10.021.

18. Østergaard, M. B., Petersen, R. R., König, J., Johra, H., Yue, Y. Z. (2017). Influence of foaming agents on solid thermal conductivity of foam glasses prepared from CRT panel glass. *Journal of Non-Crystalline Solids, 465(2),* 59–64. DOI 10.1016/j.jnoncrysol.2017.03.035.

19. Mugoni, C., Montorsi, M., Siligardi, C., Andreola, F., Lancellotti, I. et al. (2015). Design of glass foams with low environmental impact. *Ceramics International, 41(3),* 3400–3408. DOI 10.1016/j.ceramint.2014.10.127.

20. Petersen, R. R., König, J., Yue, Y. (2017). The viscosity window of the silicate glass foam production. *Journal of Non-Crystalline Solids, 456(4),* 49–54. DOI 10.1016/j.jnoncrysol.2016.10.041.

21. Arsca, S. Y., Olan, L. A. (2003). Problems of foam glass production. *Glass and Ceramics, 60(9/10),* 313–314. DOI 10.1023/B:GLAC.0000008234.79970.2c.

22. Petersen, R. R., König, J., Yue, Y. (2014). Influence of the glass–calcium carbonate mixture's characteristics on the foaming process and the properties of the foam glass. *Journal of the European Ceramic Society, 34(6),* 1591–1598. DOI 10.1016/j.jeurceramsoc.2013.12.020.

23. Jing, P. F. (2018). Review on the influence of pore characteristics on thermal conductivity of autoclaved aerated concrete. *Sichuan Building Materials, 44(2),* 11–12.

24. Østergaard, M. B., Petersen, R. R., König, J., Yue, Y. Z. (2018). Effect of alkali phosphate content on foaming of CRT panel glass using Mn_3O_4 and carbon as foaming agents. *Journal of Non-Crystalline Solids, 482(3),* 217–222. DOI 10.1016/j.jnoncrysol.2017.12.041.

25. Zhang, J. S. (1988). An approach to strength model of porous material. *Journal of Shengyang Architectural and Civil Engineering Institute, 4(3),* 10–17.

26. Chunchao, Y. L., Shan, S., Hui, Z. (2017). Brief Introduction of technical specification for application of thermal insulation & waterproofing compact system based on cellular glass. *China Building Waterproofing, 19(2),* 18–22.